Passive People Counting using Commodity WiFi

Fengyu Wang, *Student Member, IEEE*, Feng Zhang, *Member, IEEE*, Chenshu Wu, *Member, IEEE*, Beibei Wang, *Senior Member, IEEE*, and K. J. Ray Liu, *Fellow, IEEE*

Department of Electrical and Computer Engineering, University of Maryland, College Park, MD 20742
Origin Wireless Inc., Greenbelt, MD 20770 USA.

***Abstract*—Indoor people counting is crucial for many applications such as crowd control and smart building. Recent works have shown the potential of using Radio Frequency (RF) signals to estimate the occupancy level. However, most of the existing solutions require training, dense links of many devices, and usually work for only moving human subjects. In this work, we consider people counting in a quasi-static scenario and propose a non-intrusive training-free method using the Channel State Information (CSI) on a single pair of commercial WiFi devices. Different from crowd counting for moving targets that alter the environment significantly, static crowd counting is non-trivial because stationary users only produce minute changes to the wireless signals. First, we transform the quasi-static crowd counting into a continuous multi-person breathing rate estimation problem. Then we propose a novel solution, including an iterative dynamic programming and a trace concatenating algorithm that continuously track the breathing rates of multiple users. By utilizing both spectrum and time diversity of the CSI, our system can correctly extract the breathing traces even if some of them merge together for a short time period. Extensive experiments are conducted in two distinct environments (an on-campus lab and a car). The results show that our system achieves an average accuracy of 86% for both cases. For 97.9% out of all the testing cases, the absolute error of crowd number estimates is within 1.**

***Index Terms*—Multi-people breathing estimation, identity matching, crowd counting, wireless sensing.**

I. Introduction

Human-centric sensing has attracted increasing interests for a range of Internet of Things (IoT) applications [1] [2]. Demands of accurately and passively estimating the number of people (a.k.a crowd counting) in the area of interest surge for many applications. For instance, a smart home can adjust the light and ventilation system based on occupant number to improve energy efficiency [3] [4]. Similarly, being aware of how many passengers there are in a car, the intelligent transportation systems would be more efficient and responsive.

Traditional solutions mainly rely on surveillance cameras for crowd counting [5]. These vision-based approaches, however, face common limitations. For example, they are vulnerable to poor environmental lighting conditions, and a number of cameras are needed to cover an area of interests without blind spots. And importantly, all vision-based approaches raise privacy concerns.

To overcome these limitations, the community has recently made efforts in RF-based crowd counting, either in a device-based or a device-free manner. Device-based methods [6] [7] aim to count the number of user-carried wireless devices (e.g., smartphones) as the user number, which requires the users to expose their own devices to a monitor station (e.g., an Access Point) and performs badly in case a user has multiple devices. Differently, device-free RF-based approaches [8]–[14] are more attractive as it does not require the users to wear or carry any device. Past proposals, however, either rely on dense wireless links [8] and/or involve extensive training [9]–[12] to achieve crowd counting. A few works [13] [14] attempting to circumvent the need of training can only count walking targets and thus cannot work in many as important yet static/quasi-static indoor scenarios, such as offices and conference rooms.

In this paper, we propose a training-free approach for passive crowd counting using a single pair of commodity WiFi devices. Different from previous works, we are particularly interested in estimating the occupancy level in quasi-static scenarios, such as attendees in a meeting or staffs in an office. Detecting and counting static users, however, is non-trivial. First, unlike moving subjects that alter the wireless links significantly, static users only pose minute changes on the received signals. In this work, noticing that the major motion of static/quasi-static users comes from the chest movement due to respiration, we transform the quasi-static crowd counting problem into a problem of *continuous multi-user breathing rate estimation*.

Most of past proposals of breathing rate estimation [15]–[22], however, either only work for a single user [15] [16] or assume the prior knowledge of the number of users [17] [18], the exact information we aim to extract in this paper. Thus these systems cannot be directly used to estimate the occupancy level of quasi-static scenarios. To estimate user number by continuous breathing rate estimation of multiple users, we need to overcome several unique challenges.

First, a person's breathing rate varies over time, rendering it non-trivial to associate the successive breathing rate estimates to the corresponding persons. Considering that one's breathing rate will not fluctuate within a short time period, we build a Markov chain model for the natural breathing signals and further employ an iterative dynamic programming algorithm to continuously track multiple breathing traces (i.e., sequences of breathing rates of different users). By leveraging both the spectrum and time diversity of the CSI, our system can correctly extract the breathing rate traces even if some of them are merges together for a short time period.

Second, the number of users may not be fixed for an area of

978-1-7281-5503-6/20/$31.00 ©2020 IEEE

interest, since users might come and go. In order to output real-time estimates of the occupancy level, we propose to maintain the traces of existing users and concatenate the latest estimates with the presented traces to determine existing users, newly arriving users, and leaving users.

We prototype our system using a pair of commodity off-the-shelf (COTS) WiFi devices. We conduct experiments in two typical targeted environments (i.e., a lab office and a car). Extensive results show that our system is independent of environments, and the average accuracy is more than 86% for both environments. Furthermore, the system can achieve 97.9% accuracy when the absolute error of estimation is within 1 for all the testing cases. We believe the proposed approach makes an important step towards passive crowd counting and could deliver a complete solution when integrated with previous methods for moving targets.

The rest of the paper is organized as follows. We study the multi-person breathing rate estimation in Section II, followed by people counting in Section III. We present experiments in Section IV and conclude in Section V.

II. Multi-Person Breathing Rate Estimation

The channel state information (CSI) depicts how radio signals propagate from a transmitter (Tx) to a receiver (Rx). With the presence of human beings, one or more paths of signal propagation will be altered due to human motion. Given a pair of Tx and Rx with multiple omnidirectional antennas, the CSI of link m at time t and frequency f_k is modeled as

$$h_m(t, f_k) = \sum_{l=1}^{L} a_{l,m}(t)\exp(-j2\pi f_k \frac{d_{l,m}(t)}{c}) + n_m(t, f_k), \tag{1}$$

where $k \in \mathcal{V}$ is the subcarrier (SC) index with center frequency f_k in the set of usable SCs $\mathcal{V}$. L is the total number of multipath components (MPCs), while $a_{l,m}(t)$ and $d_{l,m}(t)$ denote the complex gain and propagation length of MPC l. $n_m(t, f_k)$ is the additive white noise, and c is the speed of light.

In the presence of breathing, (1) can be rewritten as

$$\begin{aligned} h_m(t, f_k) = &\sum_{i\in\mathcal{I}} \sum_{l\in\Omega_{d_i}} a_{l,m}(t)\exp(-j2\pi f_k \frac{d_{l,m}(t)}{c}) \\ &+ \sum_{l\in\Omega_s} a_{l,m}\exp(-j2\pi f \frac{d_{l,m}}{c}) + n_m(t, f_k), \end{aligned} \tag{2}$$

where $\mathcal{I}$ denotes the set of human subjects. Ω_{d_i} denotes the MPCs scattered by human being i, resulting in time-variant complex gain and delay, Ω_s denotes the MPCs that are not affected by people's breathing, whose complex gain and delay keep time-invariant. The gain of MPCs in Ω_{d_i} could be modeled as [23]

$$a_{l,m}(t) = a_{l,m} \times (1 + \frac{\Delta d_{l,m}}{d_{l,m}}\sin\theta\sin(\frac{2\pi t}{T_{b_i}} + \phi))^{-\Psi}, \tag{3}$$

where $a_{l,m}$ and $d_{l,m}$ are gain and path length in a static environment, $\Delta d_{l,m}$ is the difference of propagation length caused by chest movement, θ is the angle between human scatter and the EM wave, and ϕ is the initial phase. Ψ is the path loss exponent. Since the chest movement is much smaller than the path length, i.e., $\Delta d_{l,m} \ll d_{l,m}$, the amplitude of MPC in both Ω_s and Ω_{d_i} can be assumed to be time-invariant, e.g., $a_{l,m}(t) \approx a_{l,m}$.

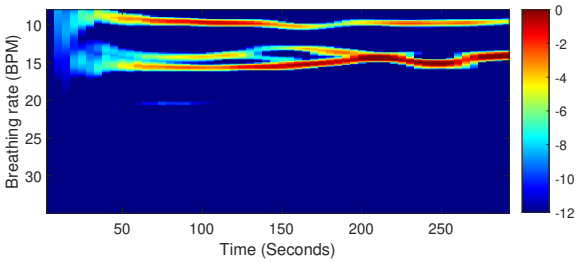

Fig. 1: Spectrogram after link combination.

It is noted that for each MPC subset Ω_{d_i}, the delay is periodic due to the periodic chest movement, i.e., $d_{l,m}(t + T_{b_i}) = d_{l,m}(t), \forall l \in \Omega_{d_i}$. Hence we would be able to see multiple frequency components of the measured CSI in frequency domain, each corresponding to a distinct breathing signal.

In order to extract breathing signals, we first apply a sliding window of length W to the captured CSI time series of each SC in every link, and then obtain the frequency spectrum by performing *Fast Fourier Transform* (FFT) over each time window. We then employ a band-pass filter on the spectrum to consider only the normal range human breathing frequencies $[b_{min}, b_{max}]$. By combining all the SCs over links, we can get a final spectrogram as shown in Fig. 1. In principle, the breathing signal is more periodic than noise and other motion interference. Thus, it is more likely to be observed as peaks in most of the time, and thus the breathing signal will form a trace in the given spectrum along the time, with the frequency changing slightly as shown in Fig. 1.

III. People Counting

A. From Breathing Rates to People Counting

Previous works estimate the number of people by the number of candidate breathing rates [21]. However, they have several limitations. First, the breathing rate estimation may not be accurate enough for a single time instance. Second, different users may have close breathing rates that are indistinguishable from the frequency spectrum, resulting in potential underestimation. Third, the number of people could vary over time as people may come and go. And the accompanying motion will also corrupt the breathing signals.

To estimate the accurate crowd number, we utilize the diversity in the time series of breathing rate estimates for reliable estimation. We first model the breathing series as a Markov Chain Model. Noting that the human breath is a periodic signal where breathing frequency can smoothly change over time, the variation of breathing rate between two adjacent time bins is assumed to follow a normal distribution $\mathcal{N}(0, \sigma^2)$, with the probability density function (PDF) $p(f)$. Since the operation of

FFT automatically discretizes the continuous frequency in the range of $[b_{min}, b_{max}]$ into $|Q|$ frequency components, where $|Q|$ means the cardinality of set Q, thus, the natural breath can be modeled as a Markov chain, and the transition probability matrix is denoted as $\mathbf{P} \in \mathbb{R}^{|Q|} \times \mathbb{R}^{|Q|}$, which is defined as

$$\begin{aligned}\mathbf{P}(q, q^{'}) &= \mathbf{P}(g(i) = q^{'} | g(i-1) = q) \\ &= \int_{(q^{'}-q-\frac{1}{2})*\Delta f}^{(q^{'}-q+\frac{1}{2})*\Delta f} p(f)\mathbf{d}f,\end{aligned} \tag{4}$$

where $\forall q, q^{'} \in Q$ and g is a mapping indicating the frequency component of the breathing rate at given time slots.

To estimate the number of people in a given time slot t, the people counting system leverages the spectrum in $[t-W, t]$, where W is the window length. An output is produced every W_s seconds, and the spectrum is updated at the same time. Thus to estimate the number of people at time t, a spectrum $S \in \mathbb{R}_+^I \times \mathbb{R}_+^{|Q|}$ is leveraged, where $I = \frac{W}{W_s}$. Since breathing signals can be observed as the visible traces in spectrogram, estimating the occupancy level is equal to counting the number of breathing traces during the observation time. In the following, we first extract the traces of successive breathing rates, and then concatenate them over time. Different from Adaptive Multi-Trace Carving (AMTC) proposed in [24], which tries to track heartbeat trace from the video signal, our algorithm can deal with the case when the number of traces changes in the adjacent time window.

B. Extracting Breathing Traces

1) Theoretical Model: For a given spectrum S, a reasonable estimate of the breathing trace can be got by

$$\mathbf{g}^* = \arg\max_{\mathbf{g}} \ E(\mathbf{g}), \tag{5}$$

where $\mathbf{g}$ indicates the breathing trace and is denoted as

$$\mathbf{g} = (g(n), n)_{n=1}^{I}. \tag{6}$$

Here $g : [1, I] \rightarrow Q$ is a mapping indicating the frequency component of the trace at the given time. $E(\mathbf{g})$ is the power of a trace defined as

$$E(\mathbf{g}) = \sum_{i=i}^{I} S(i, g(i)), \tag{7}$$

where $S(i, j)$ denotes the power at time bin i and frequency component j.

Considering that one's breathing rate will not fluctuate a lot within a short period, a regularization term should be added to penalize sudden changes in frequencies of interests. A breathing trace is then a series of breathing rate estimates that achieve good balance of frequency power and temporal smoothness. The smoothness of a trace can be evaluated by a cost function $C(\mathbf{g})$, defined as

$$\mathbf{C}(\mathbf{g}) \triangleq -\log \mathbf{P}(g(1)) - \sum_{i=2}^{I} \log \mathbf{P}(g(i-1), g(i)), \tag{8}$$

where the frequency transition probability $\mathbf{P}(g(i-1), g(i))$ can be calculated by (4). Without loss of generality, we assume a uniform prior distribution, i.e., $\mathbf{P}(g(1)) = \frac{1}{|Q|}$. The cost function $C(\mathbf{g})$ is the negative of the log-likelihood for a given trace. The smoother a trace is, the larger its probability is, and the smaller the cost it takes.

The most probable breathing trace can be found by solving

$$\mathbf{g}^* = \arg\max_{\mathbf{g}} \ E(\mathbf{g}) - \lambda C(\mathbf{g}), \tag{9}$$

where λ is a regularization factor. Here we denote $E(\mathbf{g}) - \lambda C(\mathbf{g})$ as the regularized energy of trace $\mathbf{g}$. By properly choosing the hyper-parameter λ, the people counting system can ensure that the regularized energy of a true breathing trace is positive, while when the observation area is empty, the regularized energy for any trace candidate in the given spectrum is negative.

2) Iterative Dynamic Programming: The problem in (9) can be solved by dynamic programming. However, dynamic programming typically can only find the trace with the maximum regularized energy and cannot deal with multiple breathing traces. We propose a successive cancellation scheme to find multiple traces one by one via a novel method of iterative dynamic programming (IDP).

The principle idea of IDP is intuitive. For a given spectrum S, the most probable breathing trace is first found by dynamic programming. To further determine if there are any other breathing traces, the identified trace will be erased from the spectrum, and then a new round of dynamic programming is performed to find another candidate trace. This successive cancellation procedure will be run iteratively until there is no more effective traces in the spectrum.

For clarity, (i, q) denotes the bin index with timestamp i and frequency component q. We want to find the best trace of frequency peaks from timestamp i to j, which is denoted as $\mathbf{g}_i \rightsquigarrow \mathbf{g}_j$. Define the regularized energy of trace $\mathbf{g}_i \rightsquigarrow \mathbf{g}_j$ that ends at point (j, n) as $s(\mathbf{g}_i \rightsquigarrow (j, n))$. Our approach is to search all possible traces $\mathbf{g}_i \rightsquigarrow (j, n)$ that end at frequency point n and select the best one among them. This can be achieved by finding the optimal traces for all the bins along with the adjacent timestamps. For simplicity, we denote the regularized energy at each bin as its score given by

$$\begin{aligned}s(i, q) = S(i, q) + \max_{\forall q' \in Q} \{s(i-1, q^{'}) + \lambda \log \mathbf{P}(q^{'}, q)\}, \\ i = 2, 3.., I, \ \forall \ q, q^{'} \in Q,\end{aligned} \tag{10}$$

where $s(1, q) = S(1, q) + \lambda \log \mathbf{P}(g(1) = q)$. The score of a given bin is the maximum achievable regularized energy that it can obtain. In other words, it determines the optimal paths that pass through bin (i, q).

The entire optimal breathing trace can be found by backtracking the bins that contribute to the maximum score $g^*(I)$ of the last timestamp. For the rest of the breathing trace in the observation window, i.e., $\forall \ i = I-1, I-2, ..., 1$, we have

$$g^*(i) = \arg\max_{\forall q \in Q} \ s(i, q) + \lambda \ \log \mathbf{P}(q, g^*(i+1)). \tag{11}$$

The backtracking procedure in (11) gives the optimal trace $\mathbf{g}^*$ for a given spectrum, which is the optimal solution for (9).

To further check if there are any other candidate breathing

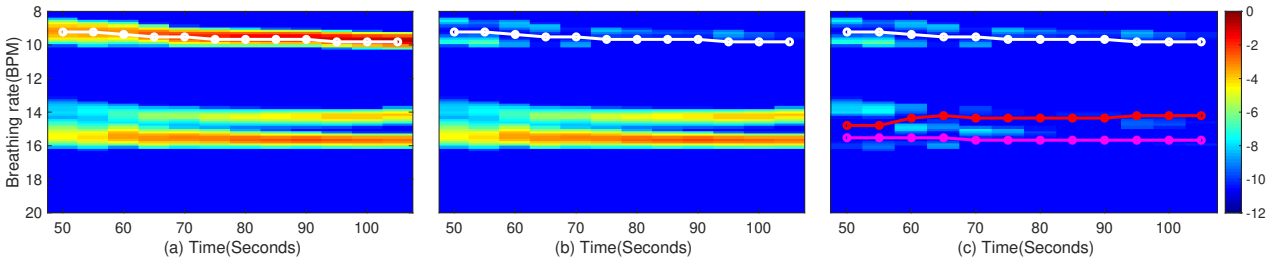

Fig. 2: Successive cancellation procedure of IDP: (a) The first trace found by IDP, (b) Spectrogram after erasing the energy stripe of first trace, (c) Spectrogram after erasing all energy stripes found by IDP.

signals in the given spectrum, the trace $\mathbf{g}^*$ should be removed. For the ideal case, we only need to remove the bins along $\mathbf{g}^*$. However, since the number of FFT points are limited, the energy of the breathing signal is diffused around the center of breathing trace, which forms an energy strip in the given spectrum as shown in Fig. 1. Thus, if we only remove the energy along the optimal trace $\mathbf{g}^*$ and consecutively execute dynamic programming in (10) and (11), we will get a group of traces inside one energy strip. Therefore, IDP applies a windowing module on the optimal trace $\mathbf{g}^*$ to emulate the diffusing effect of FFT to get an energy strip. The updated spectrum after we erase the optimal energy strip is

$$\mathbf{S}(i) \leftarrow \mathbf{S}(i) - g^*(i) * \mathbf{w}, \forall i = 1, 2, ...I, \tag{12}$$

where $\mathbf{S}(i)$ denotes the energy of spectrum at timestamp i, and $\mathbf{w}$ is the frequency response of the windowing module. Operator $*$ denotes convolution operation, which can emulate the energy stripe caused by the diffusing effect of FFT.

We recursively perform the above dynamic programming and spectrum cancellation to find multiple traces. The algorithm terminates when the score of the found trace is negative, indicating an empty spectrum without any effective traces. The procedure of iterative dynamic programming is summarized in Algorithm 1. Fig. 2 illustrates the details of this finding-then-erasing procedure. In Fig. 2 (a), the trace found by DP is marked by the line, and the energy stripe of this trace is removed as shown in Fig. 2 (b). The spectrogram, when IDP terminates, is shown in Fig. 2 (c), and lines in the figure indicate the breathing traces. It is clear to see that although there is still some residual energy not perfectly removed, IDP terminates properly since there are no traces satisfying the constraint of non-negative regularized energy.

C. Trace Concatenating

Iterative dynamic programming provides the breathing trace for each time window and determines the occupancy level based on the trace number. In practice, a continuous counting system, however, would monitor for much longer time than a time window, posing extra information gains to enhance the trace extraction. In this part, we propose a novel trace concatenating algorithm to concatenate trace segments belonging to the same breathing signal in different time windows, which not only improves the trace segments, but also enables detection of the start and end time of each trace (or equivalently, the entering and leaving time of a specific user).

Algorithm 1 Iterative Dynamic Programming

```
Calculate regularized energy map s(i, j) by (10)
Initialize trace number t ← 0, frequency response of rectangular window w
while max_q s(I, q) > 0 do
    t ← t + 1
    g_t(I) ← arg max_q g(I, q)
    i ← I − 1
    while i ≠ 0 do
        g_t^*(i) ← arg max_q  s(i, q) + λ P(q, g_t^*(i + 1))
        i ← i − 1
    end while
    update spectrum S(i) = S(i) − g^*(i) * w, ∀i = 1, 2, ...I
    Calculate regularized energy map s(i, j) by (10)
end while
```

For clarity, we store all presented traces in a database. The jth trace found previously is denoted as $\mathbf{g}_j^{\text{pre}}(t_{\text{st}} : t_{\text{end}})$, where $j = 1, \cdots, J$ and t_{st} and t_{end} denote the start and end time of the trace. The kth traces found in the current time window $[t - W, t]$ is denoted as $\mathbf{g}_k(t - W : t)$, where $k = 1, \cdots, K$. Furthermore, the similarity between two traces is defined as the ratio between the overlapped time in the window and the window length, which is expressed as

$$f(\mathbf{g}_j^{\text{pre}}, \mathbf{g}_k) = \frac{|\mathbb{1}(\mathbf{g}_j^{\text{pre}}(t_{\text{st}} : t_{\text{end}}) = \mathbf{g}_k(t - W : t))|}{I - 1}, \tag{13}$$

where $f(\mathbf{g}_j^{pre}, \mathbf{g}_k) \in [0, 1]$. A similarity matrix $F \in \mathbb{R}^J \times \mathbb{R}^K$ can be calculated according to (13) to show the similarity between all the traces in the current window and those in the database . In order to find the previous part for $\mathbf{g}_k(t - W : t)$, we only need to find the maximum item of $\mathbf{f}(\mathbf{k})$, which is the k-th column of F. The row index of the maximum similarity indicates the index of the previous trace if the maximum similarity is above a predefined threshold.

If there exists a previous trace with a high enough similarity, it means that the corresponding breathing trace has been detected before. Then the endpoint of the corresponding trace should be updated. We let the endpoint be the current time and update the corresponding frequency component accordingly. In case a new user arrives, there will be no existing traces that have a similarity larger than the threshold and thus a new trace

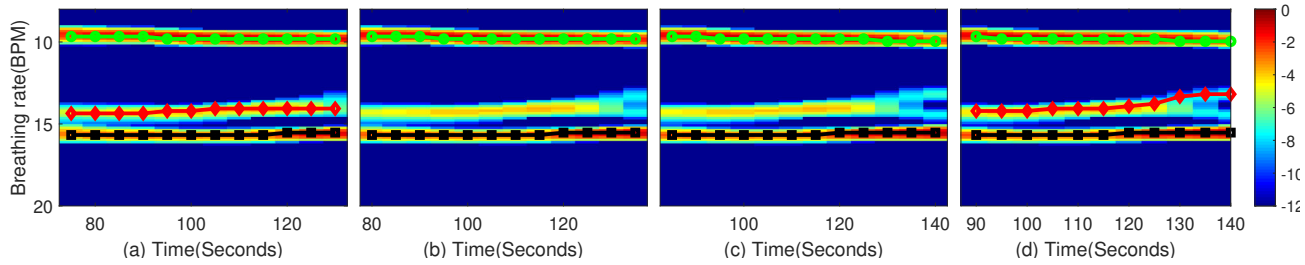

Fig. 3: Traces found by IDP in four adjacent time windows

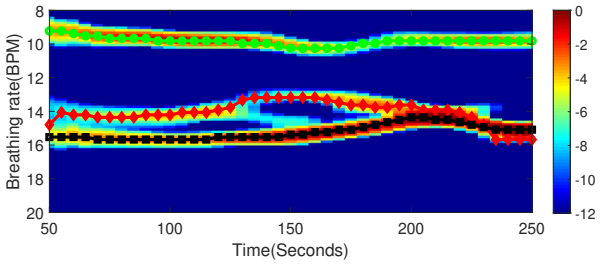

Fig. 4: Trace concatenating result of windows in Fig. 3

is created with the corresponding timestamps and frequency components. Similarly, no trace in the current window being similar to the past traces corresponds to a user that has left, and thus the trace would be terminated.

Fig. 3 and Fig. 4 show the effect of trace concatenating algorithm. Four adjacent time windows are shown in Fig. 3, and traces found by IDP are marked by lines. We can see that although the breathing trace in the middle of the spectrogram is not detected in the second and third window (due to body motion), since the trace found in the fourth window still achieves high similarity with the trace found in the first window, it still can be concatenated as shown in Fig. 4.

IV. Experiments and Evaluation

In this section, we conduct extensive experiments to evaluate the performance of the proposed approach. We conduct experiments using a pair of commodity WiFi devices, one as Tx and the other as Rx. The channel is set to 5.765 GHz with a bandwidth of 40MHz. Both Tx and Rx are equipped with 3 omnidirectional antennas. Each link between a Tx antenna and an Rx antenna has a total of 114 SCs. Considering for practical long-term monitoring, we use a very low sampling rate of 10 Hz.

All the data in our experiments are collected in an on-campus lab and a car over two months. Fig. 5 (a) shows the layout of the LAB in which two devices (Tx and Rx) are put on two different sides of a round desk located in the middle of the room, and the distance between the Tx and Rx is 3.5 m. Participants are invited to sit in chairs as if they were attending a meeting. During the experiments, the participants randomly choose their seats and slight movements are allowed. To further verify that the proposed system is independent of the environment, we also conduct experiments in a car, which is an extreme case for indoor scenario, where there is limited space as well as strong reflection. For the car scenario, the Tx

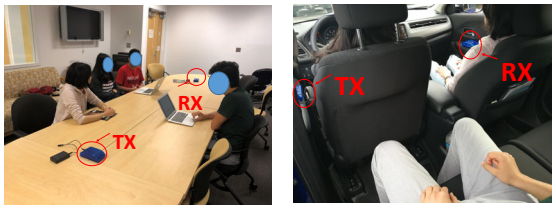

(a) LAB (b) Car

Fig. 5: Experiment setup.

and Rx are put at the front door on the driver and passenger side respectively, as shown in Fig. 5 (b).

A. Overall Performance

Fig. 6 (a) demonstrates that the confusion matrix of our method in the LAB. The counting error is within 1 for 98.6% of the testing cases. Additionally, the proposed system can perfectly detect whether the monitoring area is occupied or not. The accuracy however, decreases with more people present. This is as expected since the more people there are, the more likely their breathing traces may merge together and the more likely occasional motion may happen, both leading to counting errors. Fig. 6 (b) shows that our testing result in the car can achieve a comparable performance with that in the LAB, which demonstrates the independence of our system on the environment.

To further evaluate our system, we compare it with the most relevant TR-BREATH [21] which also estimates multi-person breathing rates. TR-BREATH employs root-MUSIC for breathing rate estimation and uses the affinity propagation algorithm to estimate crowd number. The estimation accuracy of TR-BREATH [21] is shown in Fig. 6 (c)(d). As seen, TR-BREATH shows a comparable performance in the car testing scenarios. The performance in the LAB environments is much worse, with an overall accuracy of 70.68% (mean of the diagonal elements of confusion matrix). The proposed approach improves the overall performance by 16.46% and 3.32% for LAB and car testing scenario respectively, attributed to its three core techniques: adaptive SC combination, iterative dynamic programming, and trace concatenation.

B. Impact of IDP estimation algorithm

In this section, we discuss how the proposed algorithm improves our system. Apart from the confusion matrix , here we additionally adopt true positive (TP) rate, which is calculated as:

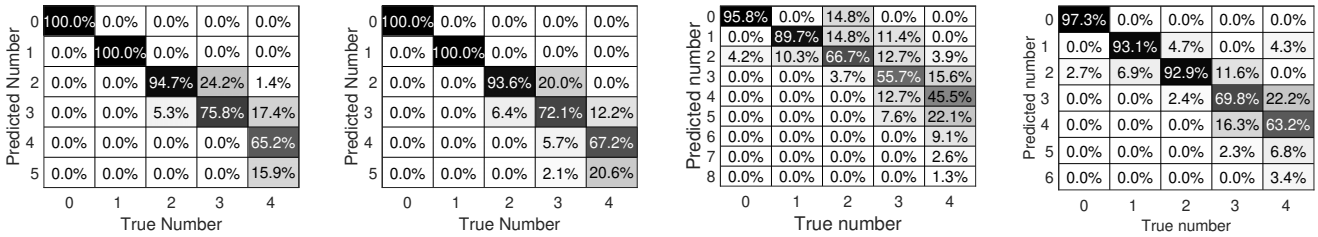

(a) Accuracy in LAB (b) Accuracy in car (c) TR-BREATH in LAB (d) TR-BREATH in car

Fig. 6: Confusion matrix of people counting

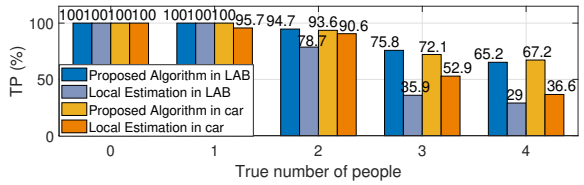

Fig. 7: TP comparison of different algorithms

$$\text{TP}_i = \frac{\#\text{ of samples that predicted label is } i}{\text{total }\#\text{ of samples that true label is } i}. \quad (14)$$

In this experiment, we show the benefits of the proposed trace tracking algorithm. We compare the performance with a *local estimation* algorithm that estimates the number of people based on the spectrum at current timestamp only. The comparisons of TP for the two algorithms are portrayed in Fig. 7. The results shows that trace tracking algorithm considerably improves the performance for both datasets, which demonstrates the gains contributed by leveraging time diversity in counting.

V. Conclusions

This paper presents a passive occupancy level estimation system for quasi-static crowds using WiFi signals. The proposed system enables static crowd counting by multi-person breathing rate estimation, which is centered by two key components: an iterative dynamic programming algorithm to extract the successive breathing traces from different individuals, and a trace concatenating algorithm that splices consecutive breathing trace segments. Experiment results show a respective average accuracy of 87.14% and 86.58% for office and car environments. Additionally, the counting error is within 1 person for 97.9% of the time.

References

[1] B. Wang, Q. Xu, C. Chen, F. Zhang, and K. J. R. Liu, "The promise of radio analytics: A future paradigm of wireless positioning, tracking, and sensing," *IEEE Signal Processing Magazine*, 2018.

[2] K.J.R. Liu and B. Wang, *Wireless AI: Wireless Sensing, Positioning, IoT, and Communications*. Cambridge University Press, 2019.

[3] S. Depatla, A. Muralidharan, and Y. Mostofi, "Occupancy estimation using only WiFi power measurements," *IEEE Journal on Selected Areas in Communications*, 2015.

[4] S. Depatla and Y. Mostofi, "Crowd counting through walls using WiFi," in *IEEE International Conference on Pervasive Computing and Communications*, 2018.

[5] Z. Al-Zaydi, B. Vuksanovic, and I. Habeeb, "Image processing based ambient context-aware people detection and counting," *International Journal of Machine Learning and Computing*, 2018.

[6] M. Soytürk, M. C. Bodur, A. B. Bakkal, and S. Öztürk, "Estimating the number of people in a particular area using WiFi," in *Signal Processing and Communications Applications Conference*, 2015.

[7] M. Wirz, T. Franke, D. Roggen, E. Mitleton-Kelly, P. Lukowicz, and G. Tröster, "Probing crowd density through smartphones in city-scale mass gatherings," *EPJ Data Science*, 2013.

[8] N. Patwari, L. Brewer, Q. Tate, O. Kaltiokallio, and M. Bocca, "Breathfinding: A wireless network that monitors and locates breathing in a home," *IEEE Journal of Selected Topics in Signal Processing*, 2014.

[9] T. Yoshida and Y. Taniguchi, "Estimating the number of people using existing WiFi access point in indoor environment," in *European Conference of Computer Science*, 2015.

[10] H. Zou, Y. Zhou, J. Yang, W. Gu, L. Xie, and C. Spanos, "FreeCount: Device-free crowd counting with commodity wifi," in *IEEE Global Communications Conference*, 2017.

[11] S. Di Domenico, G. Pecoraro, E. Cianca, and M. De Sanctis, "Trained-once device-free crowd counting and occupancy estimation using WiFi: A doppler spectrum based approach," in *IEEE International Conference on Wireless and Mobile Computing, Networking and Communications*, 2016.

[12] S. Liu, Y. Zhao, and B. Chen, "WiCount: A deep learning approach for crowd counting using wifi signals," in *IEEE International Symposium on Parallel and Distributed Processing with Applications and IEEE International Conference on Ubiquitous Computing and Communications*, 2017.

[13] S. Depatla and Y. Mostofi, "Crowd counting through walls using WiFi," in *IEEE International Conference on Pervasive Computing and Communications*, 2018.

[14] W. Xi, J. Zhao, X. Li, K. Zhao, S. Tang, X. Liu, and Z. Jiang, "Electronic frog eye: Counting crowd using WiFi," in *IEEE Conference on Computer Communications*, 2014.

[15] Y. Zeng, D. Wu, R. Gao, T. Gu, and D. Zhang, "FullBreathe: Full human respiration detection exploiting complementarity of CSI phase and amplitude of WiFi signals," *Proceedings of the ACM on Interactive, Mobile, Wearable and Ubiquitous Technologies*, 2018.

[16] F. Zhang, C. Wu, B. Wang, M. Wu, D. Bugos, H. Zhang, and K. J. R. Liu, "SMARS: Sleep monitoring via ambient radio signals," *IEEE Transactions on Mobile Computing*, 2019.

[17] H. Abdelnasser, K. A. Harras, and M. Youssef, "UbiBreathe: A ubiquitous non-invasive WiFi-based breathing estimator," in *ACM International Symposium on Mobile Ad Hoc Networking and Computing*, 2015.

[18] J. Liu, Y. Wang, Y. Chen, J. Yang, X. Chen, and J. Cheng, "Tracking vital signs during sleep leveraging off-the-shelf WiFi," in *ACM International Symposium on Mobile Ad Hoc Networking and Computing*, 2015.

[19] D. Zhang, Y. Hu, Y. Chen, and B. Zeng, "BreathTrack: Tracking indoor human breath status via commodity WiFi," *IEEE Internet of Things Journal*, 2019.

[20] C. Chen, Y. Han, Y. Chen, and K. J. R. Liu, "Multi-person breathing rate estimation using time-reversal on wifi platforms," in *2016 IEEE Global Conference on Signal and Information Processing (GlobalSIP)*, 2016.

[21] C. Chen, Y. Han, Y. Chen, H. Lai, F. Zhang, B. Wang, and K. J. R. Liu, "TR-BREATH: Time-reversal breathing rate estimation and detection," *IEEE Transactions on Biomedical Engineering*, 2018.

[22] X. Wang, C. Yang, and S. Mao, "TensorBeat: Tensor decomposition for monitoring multi-person breathing beats with commodity wifi," *ACM Transactions on Intelligent Systems and Technology*, 2017.

[23] A. Goldsmith, *Wireless communications*. Cambridge university press, 2005.

[24] Q. Zhu, M. Chen, C. Wong, and M. Wu, "Adaptive multi-trace carving based on dynamic programming," in *Asilomar Conference on Signals, Systems, and Computers*, 2018.